

Free Breathing CINE with Low Rank aided Manifold smoothness Regularization

Sunrita Poddar¹, John D Newell², and Mathews Jacob¹

¹Electrical and Computer Engineering, University of Iowa, Iowa City, IA, United States, ²Radiology, University of Iowa, IA, United States

Target Audience: MR engineers and clinicians interested in high time resolution free breathing and ungated dynamic imaging.

Purpose: Many subjects (e.g. paediatric patients, obese subjects, and subjects with compromised pulmonary function) cannot hold their breath sufficiently long for a breath-hold exam. In addition, the use of multiple breath-holds with intermittent pauses for rest results in a long scan time. In this context, methods that provide high quality images from free breathing and ungated acquisition are highly desirable.

Methods: *Manifold-smoothness free-breathing method:* We assume that the image frames in the dynamic dataset lie on a smooth low-dimensional manifold parameterized by cardiac and respiratory phases¹. The recovery of k images X_1, X_2, \dots, X_k from their undersampled measurements $A_i X_i$ is posed as the optimization problem: $X^* = \arg \min_{X_i} \|A_i X_i - b_i\|_F^2 + \sum_i \sum_j W_{ij} \|X_i - X_j\|_F^2$ (1).

Here W_{ij} are weights that are dependent on the distances between X_i and X_j on the manifold. Note that (1) is very different from binning methods^{2,3} that retain part of the acquired data to recover CINE datasets at a single or multiple respiratory phases; we reconstruct all the frames in the movie (~1000 frames from 42 seconds of acquisition time). To reduce the computational burden and memory demands when dealing with large datasets, we exploit the low rank structure of the data matrix by factorizing it as $X = UV$, where U is a matrix of spatial weights and V is a matrix of temporal basis functions. Now it is only required to store the matrices U and V . Our experiments show that 50 basis functions are sufficient to represent the signal well, which reduces the memory usage by a factor of 20. U^* and V^* are obtained by alternating minimization of (1) with respect to the unknowns.

We introduce a novel acquisition scheme (see Fig. 1) to facilitate the estimation of weights W_{ij} . For the dataset shown here, each frame was reconstructed from 10 radial lines of kspace. Each frame has 4 navigator lines acquired at the same kspace locations. The rest of the lines (6 per frame) are collected according to a continuous golden-angle acquisition. This is formalized as: $A_i X_i = \begin{bmatrix} \phi \\ B_i \end{bmatrix} X_i = \begin{bmatrix} y_i \\ z_i \end{bmatrix} = b_i$ where ϕ is the sampling operator for the navigator signals. The weights W_{ij} are then

obtained as: $W_{ij} = e^{-\frac{\|y_i - y_j\|_F^2}{\sigma^2}}$ when $\|y_i - y_j\|_F^2 < t$, and 0 otherwise, where t is a constant. The free breathing acquisition was run for 42 seconds/slice (1000 frames), which translated to a scan time of 7 minutes. The scan parameters correspond to: slice thickness=5mm, #channels=18, #slices=10, TR/TE=4.2/2.1, temporal resolution=42 ms.

Traditional Breath-held method: Breath-held and pulse oximeter triggered radial CINE data was acquired from the subject with around 20-30 s breath-hold duration (with pauses of ~45 s between slices for rest), which was reconstructed using gridding. The scan parameters correspond to: slice thickness=5mm, #channels=18, #slices=10, TR/TE=4.4/2.2. 19 phases were recovered with 192 radial views/phase.

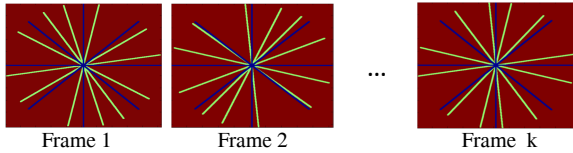


Fig 1: Kspace sampling pattern for free breathing acquisition.

$A_i X_i = \begin{bmatrix} \phi \\ B_i \end{bmatrix} X_i = \begin{bmatrix} y_i \\ z_i \end{bmatrix}$. Blue: Navigator signals obtained from same kspace locations every frame. Green: Data from different kspace locations every frame.

Red: Not sampled Green: $z_i = B_i X_i$ Blue: $y_i = \phi X_i$

Results & Discussion: 3 out of the 10 slices reconstructed are shown in Fig 2. Images from a small segment of the free-breathing reconstruction that closely matched the breath-held images are also shown. The matching of the slices was difficult due to the inconsistencies between the position of the heart in the breath-held (end-expirator) and in the free breathing mode. Good quality images are obtained with the free-breathing scheme, thus demonstrating that our method can be an alternative to breath-held schemes. We observed that some of the breath-holds were larger due to distortions in the oximeter signal, possibly due to finger motion or sweat, resulting in longer acquisitions. In our ungated free-breathing method, we eliminate the need for the ECG trigger. Our approach has similarities to², but unlike their method which reconstructs phases, we recover a time series of images.

Conclusion: We proposed a novel method for free-breathing dynamic cardiac imaging and compared it to the traditional ECG gated breath-held method. We found that good spatial and temporal resolution images were obtained with our method in a reasonable acquisition time without the need for any physiological monitors.

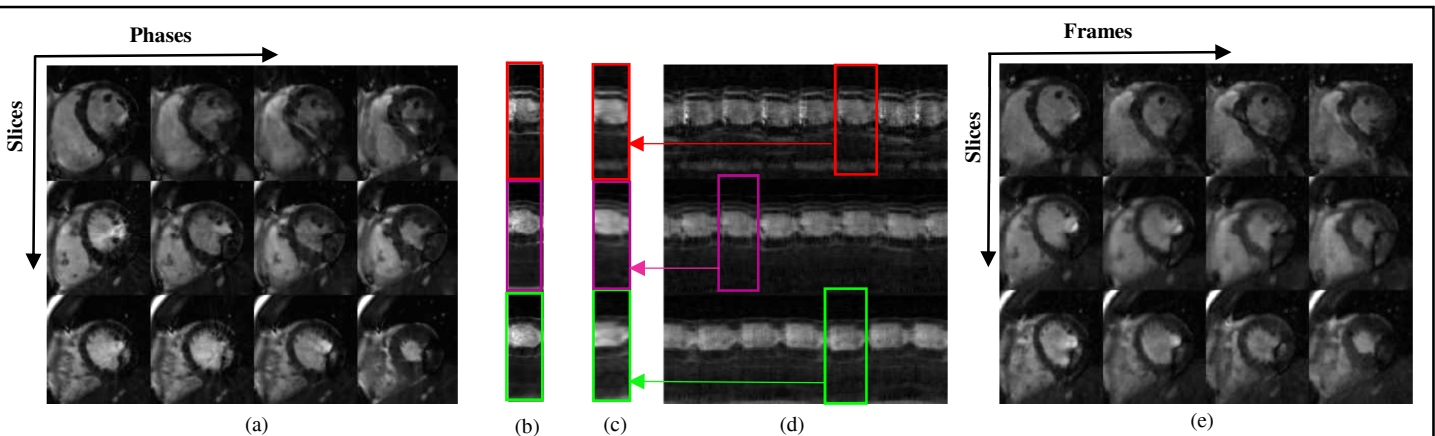


Fig 2: (a) Breath-held images (4 phases in each of 3 slices) (b) Intensity profile along a vertical cut of breath-held images plotted against phase (c) The cardiac cycle of the free-breathing images most closely matching the breath-held cycle was chosen. Intensity profile along a vertical cut of these chosen free-breathing images is shown plotted against frames (d) Intensity profile along a vertical cut of free-breathing images is plotted against frames. 7 cardiac cycles are shown here (e) Free breathing images (4 frames in each of 3 slices, that most closely match the shown breath-held phases).

References: [1] S.Poddar et al. ICASSP 2014. [2] M.Usman et al. JMIRI 2014. [3] L.Feng et al. ISMRM 2013.